THE USE OF INSTANTANEOUS PHASE FOR IMPROVING SAFT IMAGES

VANDER TEIXEIRA PRADO, RICARDO TOKIO HIGUTI, CLÁUDIO KITANO, SILVIO CESAR GARCIA GRANJA
Department of Electrical Engineering, Universidade Estadual Paulista (UNESP), Faculdade de Engenharia de Ilha Solteira
Ilha Solteira - SP, 15385-000, Brazil

ÓSCAR MARTÍNEZ-GRAULLERA
Centro de Acústica Aplicada y Evaluación No destructiva, CSIC
C/ Serrano144, Madrid, 28006, Spain

ABSTRACT: In the SAFT technique (Synthetic Aperture Focusing Technique) each element operates in pulse-echo mode, requiring only one transmit/receive channel. The generated beam pattern can present grating lobes, even if the pitch is half wavelength, which are related to image quality. By considering the instantaneous phase of the signals detected by each transducer, it is possible to estimate if the signal used in the delay-and-sum algorithm, for each combination of array element and image pixel, is due to a reflector or if it is noise, improving the contrast and reducing the grating lobes effects.
Keywords: instantaneous phase, SAFT images, grating lobes.

INTRODUCTION

When all array elements, or part of them, are excited simultaneously it is necessary a transmit/receive channel dedicated to each element, which reduces the time of data acquisition and process significantly. On the other hand, it increases the complexity and the cost of the system.

An alternative is the use of synthetic aperture techniques, in which one or a few emission and receiving channels are multiplexed, and the data is post-processed to obtain the image (Ylitalo & Ermert, 1994). In this technique the hardware complexity is reduced, without the necessity of reducing the number of elements of the aperture.

In the SAFT technique (Synthetic Aperture Focusing Technique) each element operates in pulse-echo mode, requiring only one transmit/receive channel (Thomson, 1984; Karaman et al., 1995). Post-processing dynamic focusing in emission and reception can be obtained by the delay-and-sum algorithm (DAS). However, for an array with pitch of half wavelength ($\lambda/2$), the effective aperture or coarray (Hoctor & Kassam, 1990) has λ pitch, and consequently the generated beam pattern can present grating lobes, resulting in image artifacts and reducing the contrast.

Martín et al. (2008) present the 2R-SAFT, which uses one channel in emission and two in reception, removing the grating lobes (for the case of $\lambda/2$ pitch) with the disadvantage of increasing the reception circuit complexity.

Based on Camacho et al. (2009) and Martínez-Graullera et al. (2011), that use the phase diversity at the aperture data and the spectral analysis of the phase dispersion, respectively, to improve the quality of the images, this work uses the instantaneous phase (IP) to improve the contrast and reduces the grating lobes effects in SAFT images, demanding low cost associated electronics.

Proceedings of the 2013 International Congress on Ultrasonics (ICU 2013)
Edited by Gan Woon Siong, Lim Siak Piang and Khoo Boo Cheong.
 Published by: Research Publishing
ISBN: 978-981-07-5938-4 :: doi:10.3850/978-981-07-5938-4_P0301

INSTANTANEOUS PHASE IMPROVEMENT PROCEDURE

By considering a linear array of N elements and the pulse-echo data $v_i(t)$, the transmitted/received signal by element i, the amplitude SAFT image at point (x, z) is described by:

$$I_{amplitude}(x,z) = \sum_{i=1}^{N} v_i\left(\tau_i(x,z)\right). \quad (1)$$

The use of the IP instead of the amplitude signal in the equation (1) results in the IP SAFT image:

$$I_{IP}(x,z) = \sum_{i=1}^{N} IP_i\left(\tau_i(x,z)\right). \quad (2)$$

The $IP(t)$ is obtained by calculating the phase of the analytic signal $v_{ai}(t)$. The analytic signal of $v_i(t)$ is given by (Oppenheim et al., 1999):

$$v_{ai}(t) = v_i(t) + j\hat{v}_i(t), \quad (3)$$

where $\hat{v}_i(t)$ is the Hilbert transform of $v_i(t)$.

For a point (x, z), which there is not a reflector, the IP is related to a random noise, which is uniformly distributed over 2π (Carlson & Crilly, 2009). In this case the amplitude SAFT image is multiplied by the standard deviation of the average $\bar{\sigma}$:

$$\bar{\sigma} = \frac{\sigma_0}{\sqrt{N}}, \quad (4)$$

Where σ_0 is the standard deviation of the IP noise distribution ($\pi/\sqrt{3}$). To be considered a reflector the $I_{IP}(x, z)$ must be above a threshold, which also depends on the standard deviation of the average, written as:

$$\epsilon = \sqrt{\bar{\sigma}}. \quad (5)$$

Therefore the threshold is obtained from the noise distribution and the number of elements of the array and the final image is given by:

$$I(x,z) = \begin{cases} I_{amplitude}(x,z), & if \quad I_{IP}(x,z) \geq \epsilon \\ I_{amplitude}(x,z) \,.\, \bar{\sigma}, & if \quad I_{IP}(x,z) < \epsilon \end{cases}. \quad (6)$$

POINT SPREAD FUNCTION

The point spread function (PSF) at x = 0 mm and z = 25 mm (x is the array axis centered in the middle of the array) in water (velocity of 1540 m/s) is simulated for an array of 128 elements

spaced by λ/2. A four-cycles Gaussian envelope RF signal centered in 2.4 MHz is used and a random noise with Gaussian distribution and signal-to-noise ratio of 20 dB is added to the signals.

Figure 1(a) illustrates the amplitude SAFT image, in which it is possible to observe the reflector with a lot of image artifacts due to side lobes and grating lobes, resulting in a low contrast image.

The IP image, shown in Figure 1(b), presents a smaller contrast, but the image background is approximately constant. After the application of the threshold σ = 0.4 (-7.95 dB) there is a good defect indication, which is illustrated by the binary IP image in Figure 1(c), where the presence of the reflector appears in white color and the absence of it in black. Then the amplitude image is multiplied by the standard deviation of the average ($\bar{\sigma}$ = 0.16), at the pixels considered without a reflector, reducing the image artifacts due to both side and grating lobes, improving contrast, as can be observed in Figure 1(d).

The amplitude image is multiplied by $\bar{\sigma}$ instead of zero in order to preserve some characteristics of the amplitude image. There may be cases in which the technique has low sensitivity to a reflector, for example due to the reflection coefficient. In these cases the reflector would not appear in the final image.

EXPERIMENTAL RESULTS

A phantom (CIRS model 040GSE) is experimentally examined using a 10 MHz array of 128 elements and pitch of 2λ. The solid elastic water-based polymer phantom with nylon filaments as wire targets (diameter of 80 microns) is illustrated in Figure 2. The depth of the targets is around 30 mm and the axial and lateral separations are 4, 3, 2, 1, 0.5 and 0.25 mm.

The SAFT images of the phantom can be visualized in Figure 3. It is possible to detect most reflectors, but there poor contrast and due to the presence of image artifacts some reflectors appear close to the others, not being possible to make a good identification in these cases.

With the use of the IP information, even though there are some image artifacts, the reflectors are more clearly identified and with higher contrast. Therefore the final image (Figure 3(b)) presents higher contrast and better resolution compared to the conventional amplitude SAFT image.

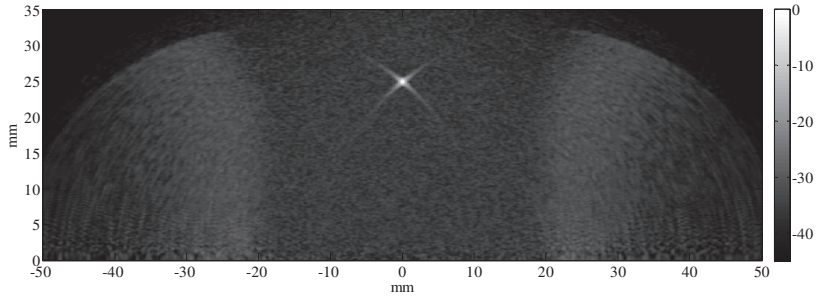

(a) Amplitude SAFT image.

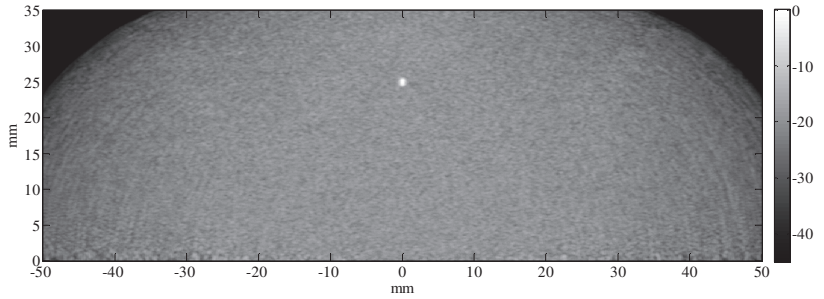

(b) IP SAFT image.

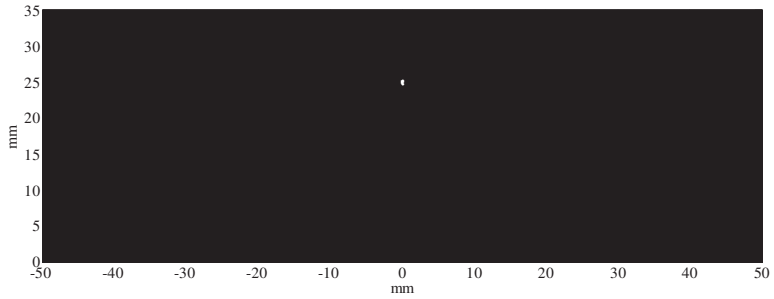

(c) Binary IP.

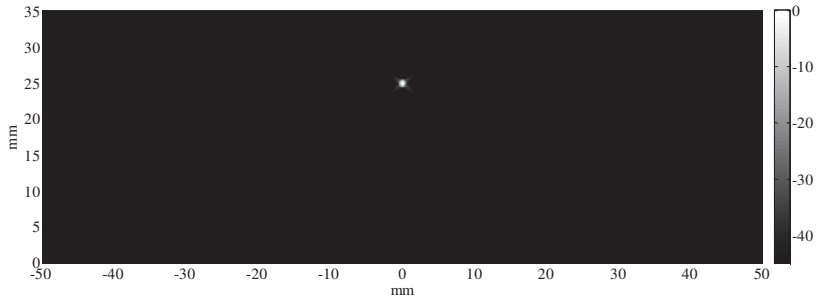

(d) Amplitude SAFT image improved by the IP.

Figure 1. PSF at x = 0 mm and z = 25 mm for SAFT: (a) amplitude image (b) IP image, (c) Binary IP (white if above threshold and black if under) and (d) amplitude image improved by the IP.

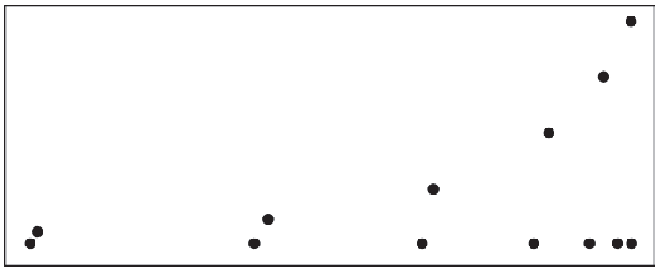

Figure 2. Phantom scheme: wire targets (diameter of 80 microns), axial and lateral separations of 4, 3, 2, 1, 0.5 and 0.25 mm.

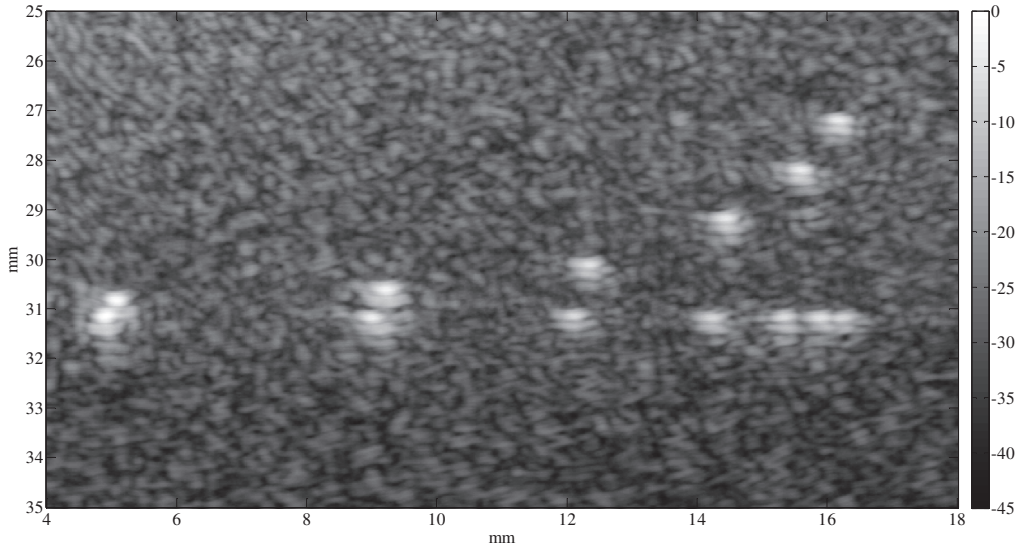

(a) Amplitude SAFT image.

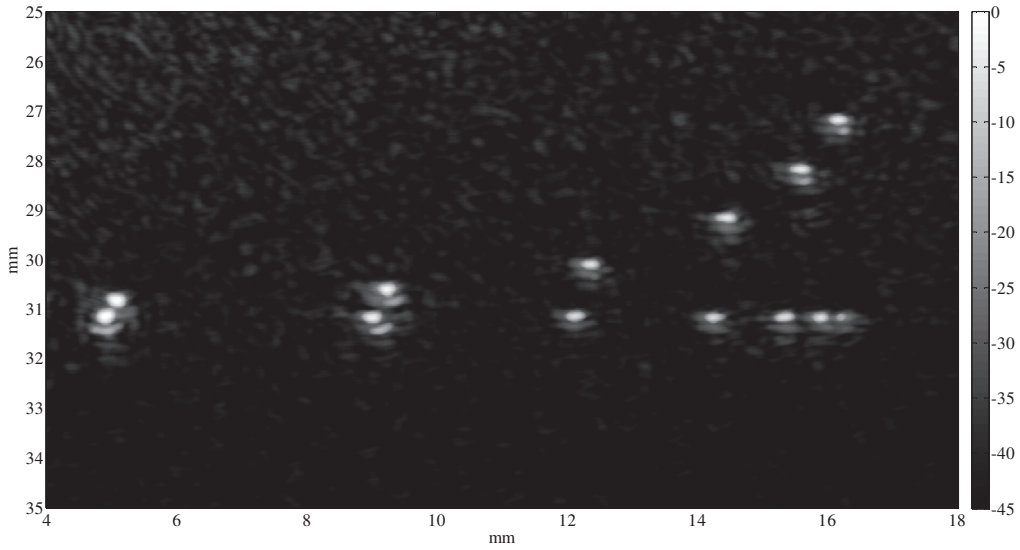

(b) Amplitude SAFT image improved by the IP.

Figure 3. Phantom: (a) amplitude SAFT image and (b) it improved by the IP information.

CONCLUSIONS

The instantaneous phase information was used to reduce grating lobes effects in SAFT images. The instantaneous phase image is thresholded by considering the standard deviation of the phase in the absence of a reflector and the number of array elements, and is then multiplied by the SAFT image. The technique has been tested in PSF simulations and using a medical phantom with an array of 128 elements at 10 MHz. As a result there is a reduction in image artifacts due to side and grating lobes, improving contrast and resolution in comparison to SAFT images.

ACKNOWLEDGMENTS

The authors would like to thank the financial support from FAPESP (2010/02240-0, 2010/16400-0), Capes and CNPq as well as the government of Spain (CICYT - DPI 2010 19376).

REFERENCES

Camacho, J., Parrilla, M. & Fritsch, C. (2009). "Phase coherence imaging", *Ultrasonics, Ferroelectrics and Frequency Control, IEEE Transactions*, 56(5), 958-974.

Carlson, A. B. & Crilly, P. B. (2009). *Communication Systems*. McGraw-Hill.

Hoctor, R. T. & Kassam, S. A. (1990). "The unifying role of the coarray in aperture synthesis for coherent and incoherent imaging", *Proceedings of the IEEE*, 78(4), 735-752.

Karaman, M., Li, P. & O'Donnell, M. (1995). "Synthetic aperture imaging for small scale systems", *Ultrasonics, Ferroelectrics and Frequency Control, IEEE Transactions*, 42(3), 429-442.

Martín, C. J., Martínez, O., Ullate, L. G., Octavio, A. & Godoy, G. (2008). "Reduction of grating lobes in saft images", *In: IEEE International Ultrasonics Symposium,*721-724.

Martínez-Graullera, O., Romero-Laorden, D., Martín-Arguedas, C. J., Ibañez, A. & Ullate, L. G. (2011). "A new beamforming process based on the phase dispersion analysis", *International Congress on Ultrasonics. Proceedings*, 1433, 185-188.

Oppenheim, A. V., Schafer, R. W. & Buck, J. R. (1999). *Discrete-Time Signal Processing*, Prentice-Hall.

Thomson, R. N. (1984). "Transverse and longitudinal resolution of the synthetic aperture focusing Technique", *Ultrasonics*, 22(1), 9-15.

Ylitalo, J. T. & Ermert, H. (1994). "Ultrasound synthetic aperture imaging: monostatic approach", *Ultrasonics, Ferroelectrics and Frequency Control, IEEE Transactions,* 41(3), 333-339.